J Comp Physiol A (1993) 173:385–399

Journal of Comparative Physiology A Sensory, Neural, and Behavioral Physiology

Local interneurons and information processing in the olfactory glomeruli of the moth *Manduca sexta*

T.A. Christensen, B.R. Waldrop*, I.D. Harrow, J.G. Hildebrand**

Arizona Research Laboratories, Division of Neurobiology, 611 Gould-Simpson-Bldg, University of Arizona, Tucson, AZ 85721, USA

Accepted: 12 April 1993

Abstract. Intracellular recordings were made from the major neurites of local interneurons in the moth antennal lobe. Antennal nerve stimulation evoked 3 patterns of postsynaptic activity: (i) a short-latency compound excitatory postsynaptic potential that, based on electrical stimulation of the antennal nerve and stimulation of the antenna with odors, represents a monosynaptic input from olfactory afferent axons (71 out of 86 neurons), (ii) a delayed activation of firing in response to both electrical- and odor-driven input (11 neurons), and (iii) a delayed membrane hyperpolarization in response to antennal nerve input (4 neurons).

Simultaneous intracellular recordings from a local interneuron with short-latency responses and a projection (output) neuron revealed unidirectional synaptic interactions between these two cell types. In 20% of the 30 pairs studied, spontaneous and current-induced spiking activity in a local interneuron correlated with hyperpolarization and suppression of firing in a projection neuron. No evidence for recurrent or feedback inhibition of projection neurons was found. Furthermore, suppression of firing in an inhibitory local interneuron led to an increase in firing in the normally quiescent projection neuron, suggesting that a disinhibitory pathway may mediate excitation in projection neurons. This is the first direct evidence of an inhibitory role for local interneurons in olfactory information processing in insects. Through different types of multisynaptic interactions with projection neurons, local interneurons help to generate and shape the output from olfactory glomeruli in the antennal lobe.

Key words: Inhibition – Local interneurons – *Manduca sexta* – Olfaction – Synaptic interactions – Antennal lobe

Introduction

The antennae of insects are their principal olfactory organs, bearing numerous cuticular sensilla innervated by receptor neurons that respond, with various degrees of sensitivity and specificity, to biologically significant odors in the environment. Information about olfactory stimuli is encoded in patterns of action potentials transmitted along the axons of the receptor neurons to the brain. There the olfactory information is amplified and integrated by olfactory interneurons, which interact synaptically in the glomerular neuropil of the antennal lobe (AL) of the deutocerebrum (see reviews by Light 1986; Christensen and Hildebrand 1987a; Rospars 1988; Homberg et al. 1989; Masson and Mustaparta 1990; Boeckh et al. 1990; Boeckh and Tolbert 1993). Synaptically processed olfactory information is transmitted to higher-order centers in the protocerebrum via output elements, the projection neurons (PNs; Homberg et al. 1988) of the AL. Previous electrophysiological investigations of PNs have revealed much about the processing of olfactory information in the brains of cockroaches (Burrows et al. 1982; Boeckh and Ernst 1987; Hösl 1990), honeybees (Homberg 1984; Arnold et al. 1988; Flanagan and Mercer 1989a, b; Sun 1991), and several species of moths (Boeckh and Boeckh 1979; Matsumoto and Hildebrand 1981; Olberg 1983; Light 1986; Kanzaki and Shibuya 1986; Christensen and Hildebrand 1987b, 1988, 1990; Christensen et al. 1989a, b, 1991; Hansson et al. 1991; Homberg et al. 1989; Kanzaki et al. 1989).

Although much has been learned about the anatomical, neurochemical, and physiological properties of various types of AL neurons and also about the synapses

* *Current address:* Department of Zoology, University of Oklahoma, Norman, OK 73019-0235, USA
** *Current address:* Animal Health Discovery, Pfizer Central Research, Sandwich, Kent, CT13 9NJ, UK

Abbreviations: AL, antennal lobe; EPSP, excitatory postsynaptic potential; GABA, γ-aminobutyric acid; IPSP, inhibitory postsynaptic potential; LN, local interneuron; MGC, macroglomerular complex; OB, olfactory bulb; PN, projection neuron; TES, N-tris[hydroxymethyl]methyl-2-aminoethane-sulfonic acid

Correspondence to: Dr. T.A. Christensen

among these elements in the ALs of moths (Tolbert and Hildebrand 1981), cockroaches (Malun 1991a, b), and honeybees (Gascuel and Masson 1991), very little is known about synaptic interactions among physiologically identified neurons in the AL, and how the olfactory responses of PNs are generated and shaped. In the sphinx moth *Manduca sexta,* the responses of PNs to electrical or odor-driven stimulation of the antennal nerve are complex and consist of both excitatory and inhibitory phases (Christensen and Hildebrand 1987b; Waldrop et al. 1987; Christensen and Hildebrand 1988, 1990). Several lines of evidence suggest that these multi-phasic responses are mediated by the second major class of interneurons residing in the AL, the amacrine local interneurons (LNs).

Various morphological types of LNs have been observed in several species of insects (Selzer 1979; Matsumoto and Hildebrand 1981; Kanzaki and Shibuya 1986; Flanagan and Mercer 1989a, b; Stocker et al. 1990; Distler 1990a). In *M. sexta,* most LNs have extensive arborizations throughout the AL, and approximately 360 of these neurons ramify throughout the array of AL glomeruli (Homberg et al. 1989). These LN arborizations overlap spatially with the projections of antennal-receptor axons and the arborizations of PNs in the glomeruli. Immunocytochemical studies have shown that many of the LNs in the AL contain γ-aminobutyric acid (GABA; Kingan and Hildebrand 1985; Hoskins et al. 1986), and this observation has since been reported for other insects as well (Schäfer and Bicker 1986; Distler 1989, 1990a). On the basis of electrophysiological and pharmacological observations, it appears that the early hyperpolarizing inhibitory postsynaptic potential (IPSP; referred to as I_1 in this report) recorded in many PNs in response to antennal-nerve stimulation is generated by these putatively GABAergic LNs (Waldrop et al. 1987; Christensen and Hildebrand 1988), but the inhibitory role of olfactory LNs has never been demonstrated directly in any species.

Many questions remain about the information-processing functions of LNs, including their roles in local-circuit interactions in the AL. In this report we analyze several heretofore undescribed physiological responses of LNs and, for the first time, describe the interactions between LNs and PNs observed by means of simultaneous intracellular recording from pairs of AL neurons. Some of this work has appeared elsewhere in preliminary form (Christensen and Hildebrand 1986).

Materials and methods

Preparation. Adult *Manduca sexta* (Lepidoptera: Sphingidae), up to 5 days post-eclosion, were used for all experiments. Details of dissection and methods of preparing the moths for intracellular recording have been published elsewhere (Christensen and Hildebrand 1987b). After the AL had been desheathed with fine forceps, the preparation was superfused with physiological saline solution containing (in m*M*) 150 NaCl, 3 $CaCl_2$, 3 KCl, 10 TES (N-tris[hydroxymethyl]methyl-2-aminoethane-sulfonic acid) buffer, and 25 sucrose (pH 6.9, modified from Pichon et al. 1972).

Intracellular recording and stimulation. Electrodes were filled with one of several solutions: (1) 3 *M* KCl, (2) 2 *M* K-acetate, (3) 150 m*M* hexammine cobaltic chloride (Sigma) in 1 *M* K-acetate, or (4) 4% (w/v) Lucifer Yellow CH (Aldrich) in distilled water. Injection of Lucifer Yellow or cobalt followed standard procedures (e.g. Christensen and Hildebrand 1987b).

Four types of stimulation were used to generate postsynaptic responses in AL neurons: (1) electrical stimulation of the antennal

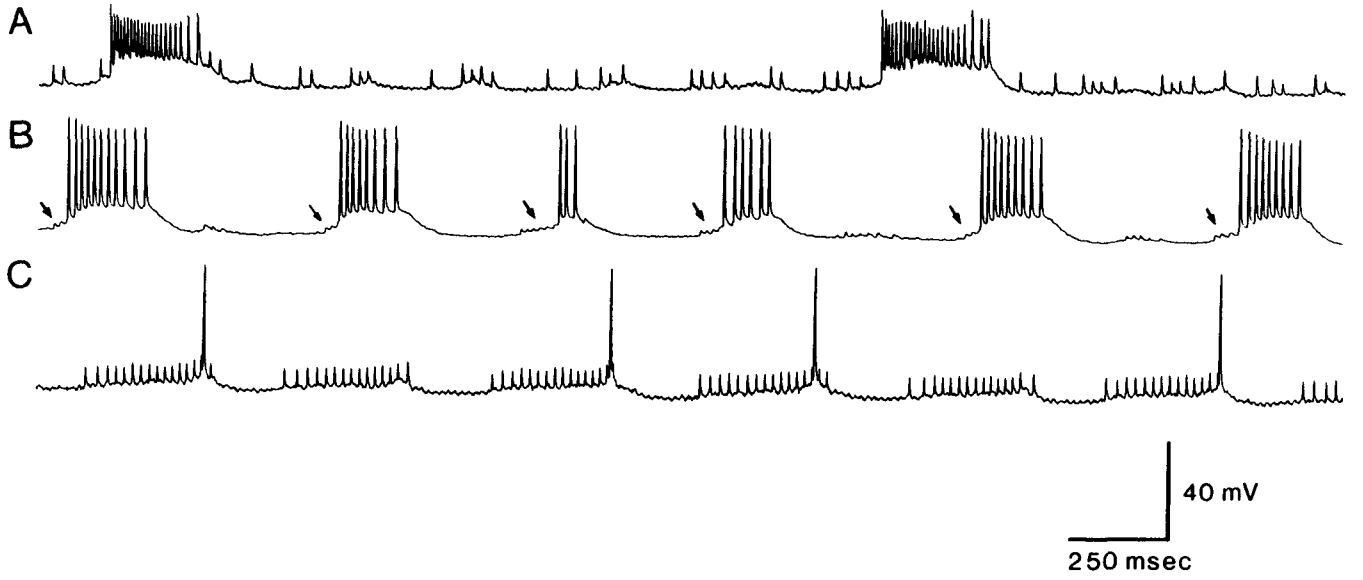

Fig. 1A–C. Spontaneous activity of LNs in *M. sexta.* More than 75% of LNs exhibited spontaneous activity, and recordings from LNs typically included spikes of more than one amplitude. **A** This neuron received strong, periodic excitatory input that resulted in depolarizations leading to bursts of large-amplitude spikes. Clusters of 3 or 4 small-amplitude spikes appeared out of phase with the bursts of large-amplitude spikes. **B** Small, subthreshold depolarizations *(arrows)* preceded each of the larger depolarizations that led to bursts of large-amplitude spikes. **C** This neuron exhibited regular bursts of small-amplitude spikes. A large-amplitude spike often occurred at the end of the burst when the membrane became more depolarized

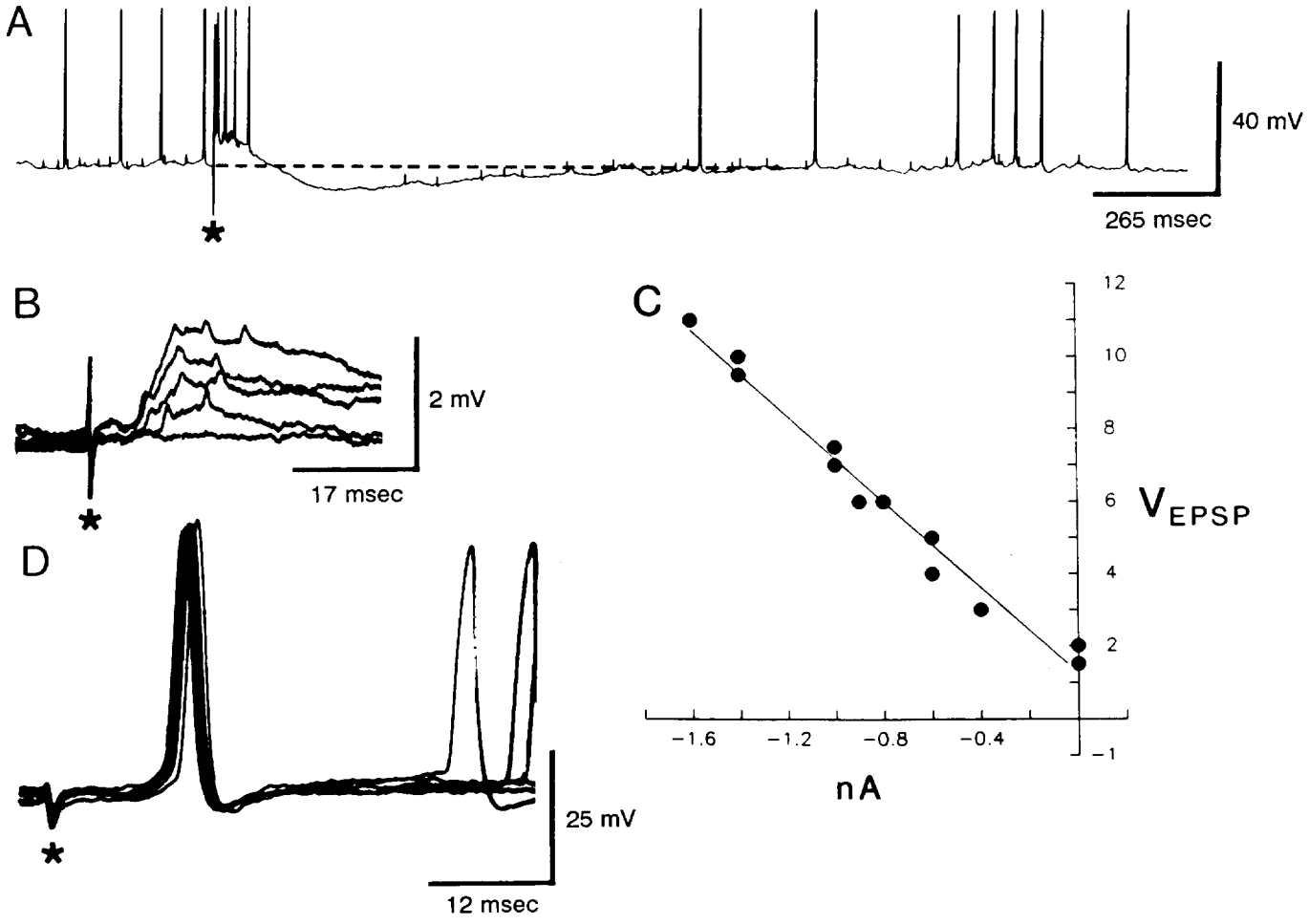

Fig. 2A–D. Short-latency excitatory responses in LNs elicited by electrical stimulation of the ipsilateral antennal nerve. In this and subsequent figures, stimulus artifacts are indicated by an *asterisk*. **A** A typical response consisted of a rapid-onset depolarization, which led to an increase in the frequency of large-amplitude spikes, followed by a prolonged (> 1 s) hyperpolarization during which all firing was temporarily suppressed. Note that small-amplitude spikes recovered first, followed by the large-amplitude spikes. *Dashed line* indicates resting membrane potential. **B** Superimposed traces showing changes in EPSP amplitude and latency evoked by 1-, 5-, 10-, 15-, and 20-V shocks. **C** Plot of amplitudes of antennal nerve-evoked EPSPs vs. injected hyperpolarizing currents. **D** Superimposed traces showing responses in another LN to suprathreshold shocks delivered to the antennal nerve. Stimuli at 20 Hz elicited large-amplitude spikes, which followed with a short and consistent latency, suggesting a monosynaptic input from antennal primary afferents

nerve, (2) mechanical stimulation of the antenna, (3) olfactory stimulation of the antenna, and (4) in double-impalement experiments, injection of current into one neuron through an intracellular microelectrode while the activity of the other neuron was monitored simultaneously with a second intracellular microelectrode. Stimulation procedures are described in detail elsewhere (Christensen and Hildebrand 1987b; Christensen et al. 1989b). When odorants were used, the antenna to be stimulated was ventilated continually with a steady stream of charcoal-filtered air. A pulse of air from the continuous airstream was diverted via a solenoid-activated valve (General Valve Corp.) through a glass cartridge bearing the stimulus on a piece of filter paper. The duration of every odor presentation was constant for a given experiment. Across all experiments, the stimulus duration was between 400–500 ms. Olfactory stimuli were: (1) *n*-hexane dilutions of the plant-associated volatiles (*E*)-2-hexenal, 1-hexanol, benzaldehyde and amyl acetate, (2) crushed tobacco leaves (a natural host plant of *M. sexta*), (3) extracts of the female moth's sex-pheromone gland (prepared by dipping an abdominal tip in 60 µl of *n*-hexane for 1 min), and (4) dilutions of synthetic (*E,Z*)-10,12-hexadecadienal (bombykal), the principal component in the natural sex-pheromone blend of *M. sexta*, in *n*-hexane (Starratt et al. 1979; Tumlinson et al. 1989). Purified bombykal was kindly provided by J.H. Tumlinson, USDA, Gainesville, FL.

Extracellular recording. Conduction velocity along a 2-mm length of antennal nerve was measured by recording orthodromic spikes generated by extracellular electrical stimulation. Two pairs of bipolar silver wires (10 µm in diameter) were fashioned into hooks and served as stimulating and recording electrodes. The wires were insulated except where they contacted the antennal nerve. Electroantennograms (EAGs), as used previously (Christensen and Hildebrand 1987b), were recorded from antennae during experiments involving stimulation with odors, in order to monitor the time course of receptor cell activation.

Data analysis. All electrophysiological data were recorded on FM tape for subsequent off-line analysis. Analog data were collected by an 80286-based micro-computer equipped with a Data Translation DT2801 data-acquisition board. Spike-triggered averages of intracellular postsynaptic potentials and cross-correlation analysis of paired recordings were obtained with customized ASYST scientific

software programs (Keithly Instruments, Rochester, NY) and plotted with a Hewlett-Packard 7470 plotter.

Results

General physiological characteristics of LNs

LNs were impaled with microelectrodes directed into the center of the AL, where the large-diameter principal neurites of LNs are found in the coarse central neuropil (Matsumoto and Hildebrand 1981). Recordings were obtained from 38 neurons, which were also stained intracellularly by injection of dye and subsequently identified as LNs, and from 48 other neurons that exhibited physiological characteristics very similar to those of the stained LNs (Table 1).

LNs had resting potentials between -50 and -60 mV, as measured with microelectrodes filled with 2 *M* K-acetate. All LNs supported large and sometimes overshooting action potentials with a mean amplitude of ca. 45 mV (range 30–80 mV) (Fig. 1). The time-course of LN spikes was notably different from that measured in PN spikes. The mean half-width of spikes in 10 randomly selected PNs was 1.2 ± 0.1 ms (S.E.M.), whereas the mean half-width of spikes in 10 randomly selected LNs was about twice that value (2.3 ± 0.2 ms).

In many LN records, smaller all-or-none potentials with rapid rise- and decay-times and maximum amplitudes of 5–20 mV were also visible (Fig. 1A and C). Small-amplitude spikes were clearly distinct from smaller, subthreshold potentials of variable amplitude, which were also readily visible in the neuropil recordings (Fig. 1B, arrows). Small-amplitude spikes were first described in LNs by Matsumoto and Hildebrand (1981) who proposed that they may represent attenuated spikes generated in electrically remote compartments (e.g., perhaps the more distal dendritic regions) of these multiply branched neurons. Although it is possible that these potentials arise from another neuron, several lines of evidence indicate that this is not the case. First, these small spikes have not been observed in recordings from other cell types, such as PNs (see below). Second, they have been observed in hundreds of cases in which subsequent staining revealed that a single neuron had been penetrated (Matsumoto and Hildebrand 1981; see below). Third, gap junctions between neurons have not been observed in olfactory neuropil (Tolbert and Hildebrand 1981), nor has dye-coupling been observed (with Lucifer Yellow as intracellular stain – see below).

More than 75% of all LNs exhibited spontaneous excitatory activity, but different patterns of activity were observed. Some neurons exhibited mainly small-amplitude spikes (Fig. 1C), while in others, large-amplitude spikes were predominant (Fig. 1B). In most cells, however, brief bursts of both small- and large-amplitude spikes were observed (Fig. 1A). Furthermore, in these cells, the occurrence of large-amplitude spikes appeared to be independent of the small-amplitude spikes (Figs. 1A and 2A). In a few neurons, such as the one shown in Fig. 1C, the membrane depolarizations were more regular, resulting in periodic bursts of spikes at nearly fixed intervals.

Synaptic input to LNs from antennal receptor neurons

Three patterns of postsynaptic responses were revealed in LNs by electrical stimulation of the antennal nerve: (1) short-latency depolarization with activation of firing, (2) delayed depolarization with activation of firing, and (3) delayed hyperpolarization with suppression of firing (Table 1). In the following sections, the physiological

Table 1. Summary of the types of local interneurons from which recordings were obtained

Physiological response	Pattern of arborization			
	symmetrical	asymmetrical	not identified	row totals
short-latency+[a]	24	2	45	71
delayed+	11	0	0	11
delayed−	0	1	3	4
column totals	35	3	48	86

[a] *Short-latency* is defined here as an excitatory response with a 0.5–2 ms latency, and a *delayed* response is one with a latency > 5 ms, after correction for antennal-nerve conduction time of 5–6 ms

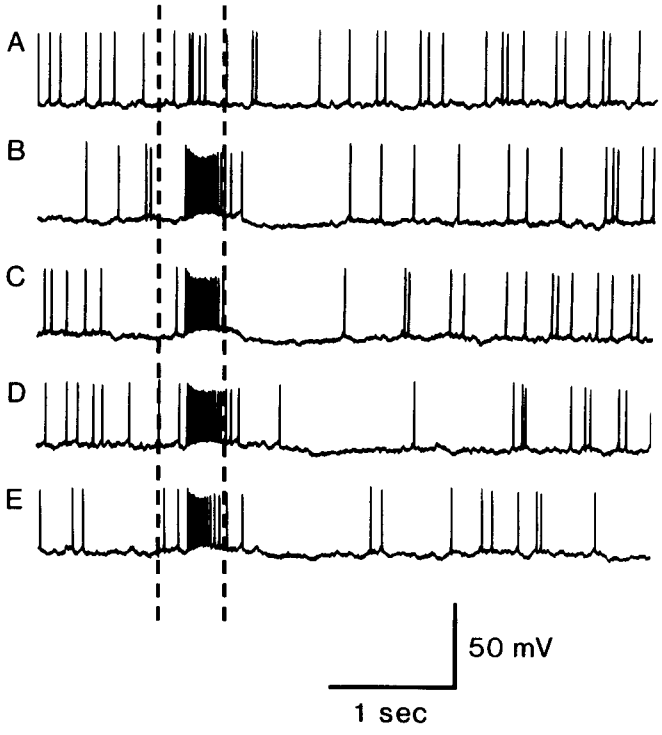

Fig. 3A–E. Responses of a short-latency excited LN in a female to olfactory stimulation of the ipsilateral antenna with plant odors. The *vertical dashed lines* indicate onset and duration of stimulus airflow. The temporal characteristics of these responses were similar to those of the electrically driven responses (Fig. 2A). **A** *n*-hexane blank; **B** (*E*)-2-hexenal, 420 µg; **C** 1-hexanol, 410 µg; **D** benzaldehyde, 520 µg; **E** isoamyl acetate, 440 µg. All stimuli were applied to filter-paper strips and loaded into glass cartridges (see Methods)

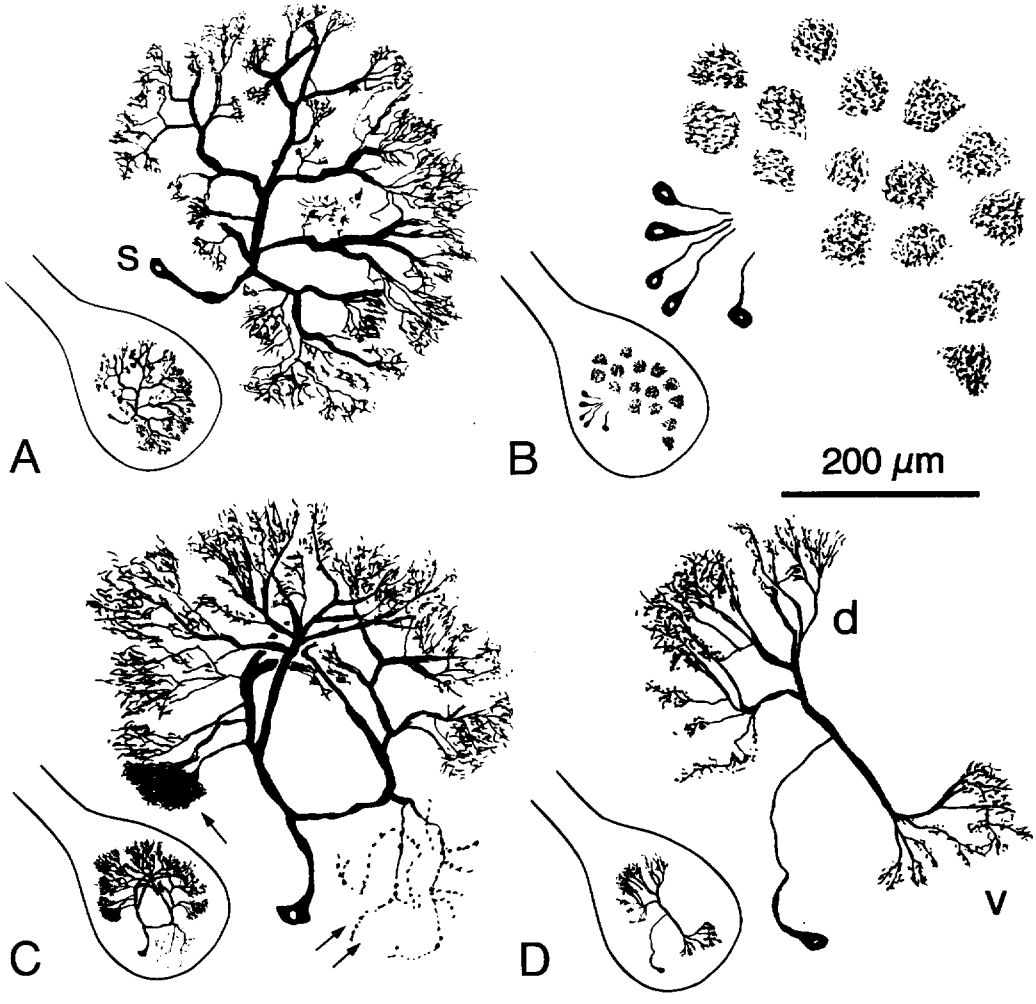

Fig. 4A–D. Morphologies of LNs in females exhibiting short-latency excited responses, reconstructed in frontal view, with the aid of a camera lucida, after intracellular staining with hexammine cobaltic chloride. Insets show positions of the neurons in the AL. **A** A typical symmetrical LN had arborizations throughout the AL glomeruli. The soma (*s*) resided in the lateral cell group. **B** A preparation in which 5 symmetrical LNs were stained simultaneously. The dense arborizations of these LNs defined the boundaries of individual glomeruli. **C** An asymmetrical LN with dense arborizations in one glomerulus *(arrow)*, less dense arborizations in dorsal glomeruli, and very sparse arborizations in ventro-medial glomeruli *(double arrow)*. The soma was in the lateral cell group. **D** An asymmetrical LN with only 2 localized fields of arborizations. The larger dorso-lateral field (*d*) was near the entrance of the antennal nerve into the AL, while the smaller field (*v*) was in the ventro-lateral region of the AL

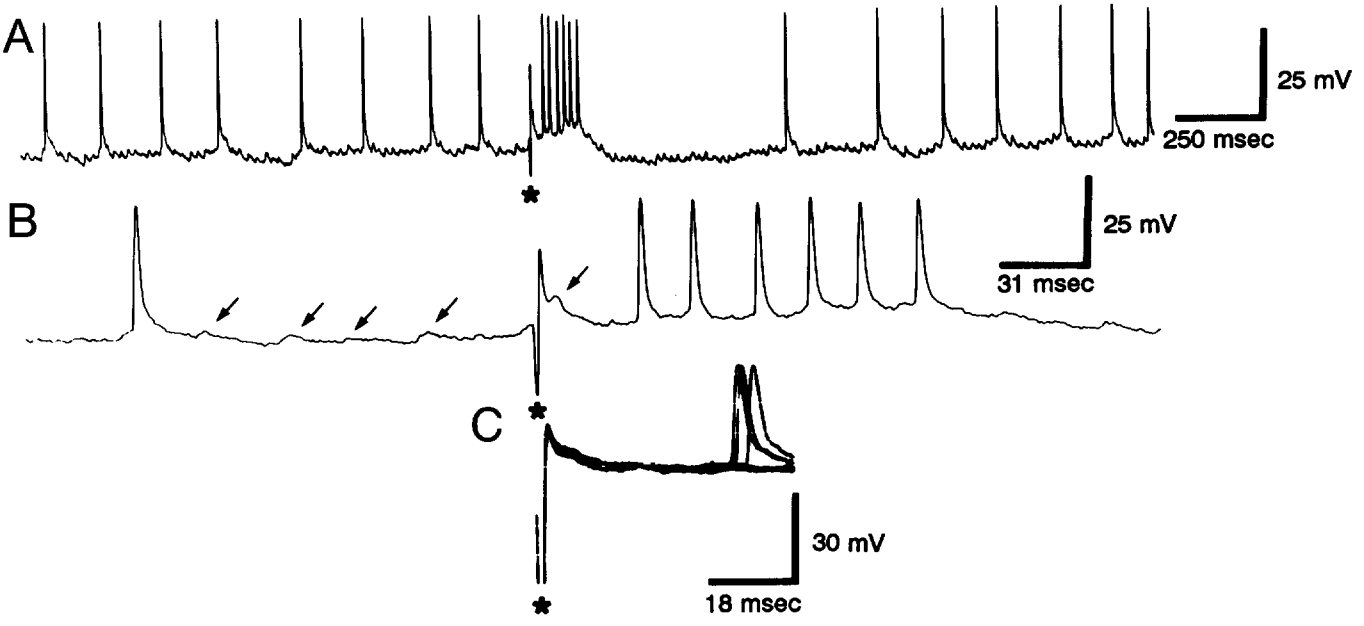

Fig. 5A–C. Delayed-input excitatory responses in LNs elicited by electrical stimulation *(asterisk)* of the antennal nerve. **A** The response consisted of delayed spiking activity followed by hyperpolarization and cessation of firing. **B** On a faster time scale, the latency to the first spike can be seen to have been ca. 36 ms (after subtraction of conduction time) from the onset of the stimulus artifact. Small depolarizations resembling EPSPs are indicated by *arrows*. **C** Repeated stimulation showed that no events were phase-locked to the stimuli when they were delivered at 10 Hz. A delayed spike was elicited by the first 3 out of 5 stimuli, and these spikes had variable latencies

characteristics of each pattern are outlined, followed by a description of the morphology of representative LNs revealed by intracellular staining.

Short-latency excitatory response

Physiology. By far the most common LN response (71 out of 86 neurons) began with membrane depolarization and a brief period of firing, followed by a moderate or sometimes prolonged period of hyperpolarization during which firing was suppressed (Fig. 2A). Antennal-nerve stimulation that was subthreshold for generation of large-amplitude spikes evoked a depolarizing potential with characteristics of a compound excitatory postsynaptic potential (EPSP). The latency of the EPSP decreased with increasing stimulus intensity, and its amplitude was graded with stimulus intensity (Fig. 2B). Using a fixed stimulus intensity, the EPSP increased linearly with injection of hyperpolarizing current (Fig. 2C), which indicates chemical synaptic input. At greater stimulus intensities, the EPSP evoked a large-amplitude spike (Fig. 2D). Tests for monosynapticity showed that this spike occurred at a relatively fixed latency, followed 1:1 with each electrical stimulus delivered to the antennal nerve, and did not fluctuate at stimulation frequencies up to 20 Hz (Fig. 2D).

In response to antennal nerve stimulation, the initial depolarization was followed immediately by a prolonged hyperpolarization during which all firing was suppressed (Fig. 2A). In the response shown in Fig. 2A, note that during the hyperpolarization, the small-amplitude spikes recovered ca. 635 ms before the large-amplitude spikes, again suggesting that these 2 types of action potentials are generated in different parts of the neuron.

Responses to odors. The responses of 12 short-latency, excited LNs to antennal stimulation with odors were also recorded in 12 female moths. Ten of these LNs were not affected by a mechanosensory stimulus (blank), and the other 2 displayed a weak response as in Fig. 3A. We did not test sex pheromones in these preparations because previous studies had revealed a lack of responsiveness to pheromones in AL interneurons in females (Matsumoto and Hildebrand 1981). Plant volatiles, on the other hand, elicited complex excitatory/inhibitory responses similar to those evoked by electrical stimulation of the antennal nerve (compare Figs. 2A and 3B–E). These odor-driven responses displayed little variability from neuron to neuron. None of the 12 LNs showed selectivity for any of the stimuli tested, and the responses elicited by (*E*)-2-hexenal, 1-hexanol, benzaldehyde, and isoamyl acetate all had similar temporal characteristics (Fig. 3B–E, respectively). The 150–200 ms latency to membrane depolarization (165 ms in Fig. 3B) was much longer than that observed in responses evoked by electrical stimulation of the antennal nerve (Fig. 2) and was attributable to the passage of odor molecules from the stimulus apparatus to the antennal receptors. It should be noted that latency measurements from odor-driven responses are

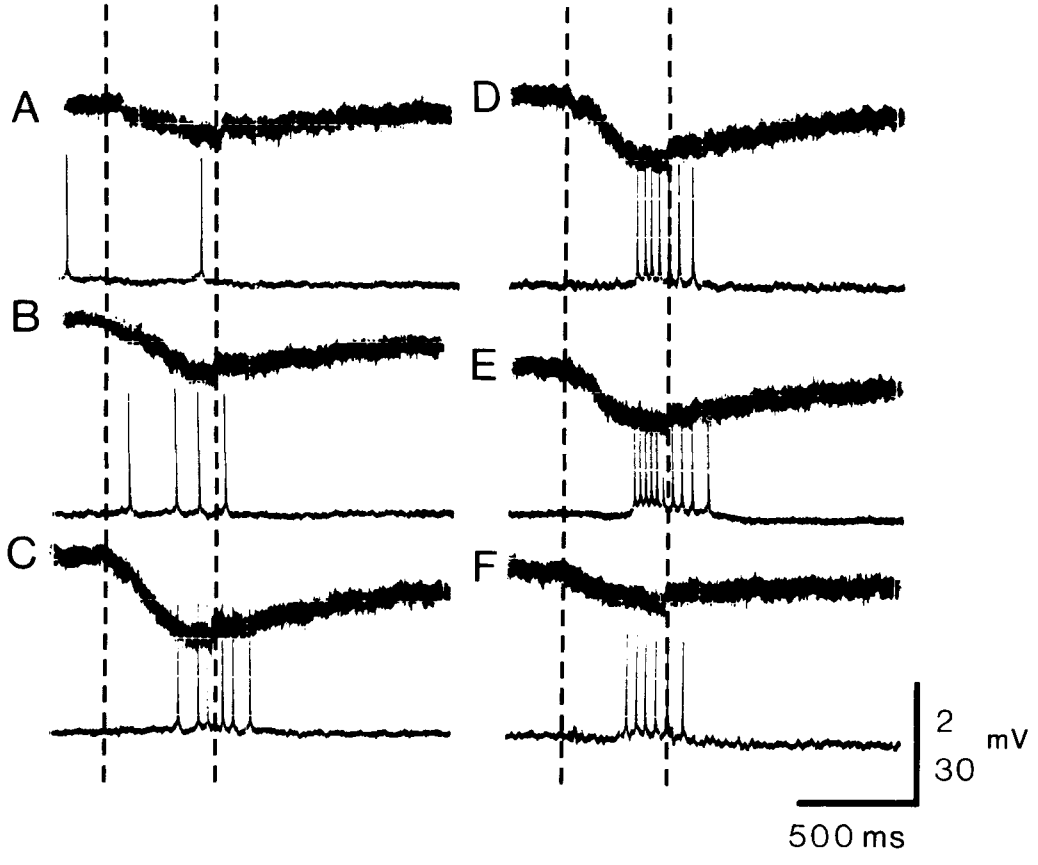

Fig. 6A–F. Responses of a delayed-input excited LN in a male to stimulation of the ipsilateral antenna with various odors. In each case, the *top trace* is an electroantennogram (EAG) recording, and the *lower trace* is the intracellular record from the LN, recorded simultaneously with the EAG. The *vertical dashed lines* indicate onset and duration of stimulus. **A–C** Different levels (1 ng, 5 ng, and 50 ng, respectively of the major sex-pheromone component, bombykal. **D** Response to 1 female equivalent of pheromone-gland extract. **E** Response to volatiles from crushed tobacco leaf. **F** Response to (*E*)-2-hexenal, a common plant aldehyde, 8 μg. In all cases, the latency between the onset of the EAG and the onset of the intracellular response was 200–300 ms. Note different vertical scales for EAG *(upper)* and intracellular *(lower)* records

difficult to quantify due to factors such as the natural turbulence in the stimulus airflow and the response characteristics of the olfactory receptor neurons.

The evoked membrane depolarization produced a train of spikes that approximately matched the duration of the stimulus and then abruptly was halted by a membrane hyperpolarization and prolonged period of inhibition. Firing was almost completely suppressed for up to 2 s during this period of inhibition before background levels of activity resumed.

In addition to the odor responses recorded from females, the response of one unstained LN in a male to the natural pheromone component bombykal was recorded during the simultaneous impalement of one LN and one PN (see below). This LN responded to electrical stimulation of the antennal nerve with a similar excitatory/inhibitory response as shown in Fig. 2A. In contrast to the complex excitatory/inhibitory responses elicited by plant volatiles, however, this single pheromone component evoked only the membrane hyperpolarization and suppression of ongoing spike activity (see Fig. 11C and text below). We did not test other odors to determine if they might drive the excitatory input to this cell.

Morphology. The most common morphological type of LN in *M. sexta* was originally described as "symmetrical" on the basis of its pattern of arborization in the AL glomeruli (Matsumoto and Hildebrand 1981). In accordance with this finding, most LNs in this study that exhibited short-latency excitatory input and were also stained (24 out of 26) had a wide-field, symmetrical pattern of branching throughout the AL. Only 3 of these 24 neurons were stained in males, and none of these had arborizations in the male-specific macroglomerular complex (MGC).

Some variation in the branching patterns of symmetrical LNs was observed, but we have not yet studied a symmetrical LN that appeared to be uniquely identifiable in males or females. Every LN had its soma in the lateral group of AL neurons. The primary neurite, which often was characterized by at least one distinct swelling, branched in several places, and each major branch sent processes into approximately the same number of glomeruli. Most if not all of the glomeruli were innervated by the secondary and tertiary branches of these neurons (Fig. 4A). The extent to which LN processes ramified throughout individual glomeruli was revealed in preparations in which several symmetrical LNs had been stained extracellularly and simultaneously (Fig. 4B). The arborizations were very dense and appeared to extend throughout each glomerulus but not into the neuropil immediately surrounding it.

Two additional LNs (in females) showed markedly "asymmetrical" branching patterns (Matsumoto and Hildebrand 1981). One had arborizations throughout the AL but ramified sparsely in the ventro-medial glomeruli and relatively densely in a single lateral glomerulus (Fig. 4C). Another LN had only 2 major arborization fields (Fig. 4D): one in the ventro-medial part of the AL and the other in a larger area of the dorso-lateral to dorso-medial part of the AL. Other regions of the AL lacked arborizations of this neuron (Fig. 4D). Thus we found several morphological types of LNs exhibiting the short-latency excitatory response, but the neurons with global, symmetrical arborizations in the AL were the most frequently encountered.

Delayed excitatory response

Physiology. The response of 11 LNs to electrical stimulation of the antennal nerve was a brief burst of spikes, followed by membrane hyperpolarization and temporary suppression of firing (Fig. 5A). Again, spontaneous depolarizations (arrows in Fig. 5B) and large-amplitude spikes were visible in the same record. In 3 cells, such as the neuron shown in Fig. 1C, small-amplitude and large-amplitude spikes were observed in the same recording. In contrast to the responses described above, however, the latency to the first large-amplitude spike evoked by elec-

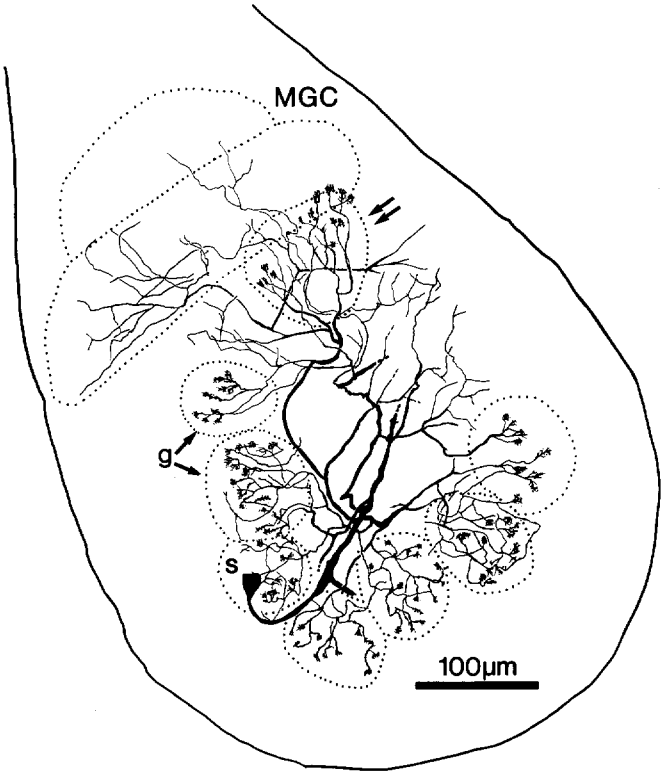

Fig. 7. Morphology of a delayed-input excited LN in a male, reconstructed in frontal view after intracellular staining with hexammine cobaltic chloride. Only the most anterior arborizations are shown. Approximate outlines of the ordinary, spheroidal glomeruli (*g*) and the macroglomerular complex (*MGC*) are indicated by *dotted lines*. A glomerulus that is adjacent and posterior and ventral to the MGC is indicated by the *double arrows*. The LN's soma (*s*) was in the lateral group of AL cell bodies. The anterior branch of the primary neurite split into secondary and tertiary branches, which divided further into very fine tufts of neurites as they invaded many of the glomeruli throughout the AL. Such a pattern of arborization has been described as "symmetrical" because each major neurite has arborizations in approximately the same number of glomeruli. This neuron also sent processes into the lower subdivision (the toroid, Hansson et al. 1991) of the male-specific MGC

trical stimulation was variable and longer than 20 ms in every neuron. Moreover, the spikes elicited did not follow (1:1) electrical stimulation of the antennal nerve at 10 Hz (Fig. 5C). These characteristics are consistent with a polysynaptic input or delayed activation of firing in these LNs, but such responses may also reflect direct synaptic input that is electrically remote from the site of impalement (see Discussion).

Responses to odors. The odor-evoked responses of 5 of these LNs were also qualitatively and quantitatively different from the responses observed in the LNs already described. All odor-evoked responses were excitatory, but considerably fewer spikes were elicited, and the latency to the first impulse was more delayed than in the LN responses described previously (compare Fig. 3 with Fig. 6B–F). The delay between the onset of the EAG response (upper traces in Fig. 6A–F) and the onset of the membrane depolarization was 200–300 ms, but again, these latency measurements are only approximate. The strongest odor stimuli, reflected in the amplitude of the EAG responses, elicited only a small depolarization that produced no more than 10 spikes (Fig. 6C–D). There was little or no hyperpolarization following the period of excitation. Considerable convergence of olfactory information was evident in the neuron (from a male moth) shown in Fig. 6, which responded in a qualitatively similar fashion to antennal stimulation with female sex pheromone (Fig. 6A–D) and with plant odors (Fig. 6E–F).

Morphology. A camera-lucida reconstruction of the LN described in Fig. 6 that received delayed excitatory input is shown in Fig. 7. Again, the cell body was located in the lateral cell group of the AL. The primary neurite branched in a symmetrical fashion and had arborizations throughout the AL, presumably in all of the glomeruli including the male-specific MGC. The symmetrical pattern of branching throughout the "ordinary" glomeruli was similar to that of the symmetrical short-latency excited LNs (Fig. 4A and B), but only the most anterior arborizations are shown for clarity.

Delayed inhibitory response

Physiology. In 4 LNs, the first event in response to electrical stimulation of the antennal nerve was not membrane depolarization but instead a delayed hyperpolarization during which firing was completely suppressed for 200–250 ms (Fig. 8A). The latency to the hyperpolarization was greater than 5 ms, indicating that the input from antennal-nerve afferents was probably polysynaptic. The membrane hyperpolarization appeared to be a com-

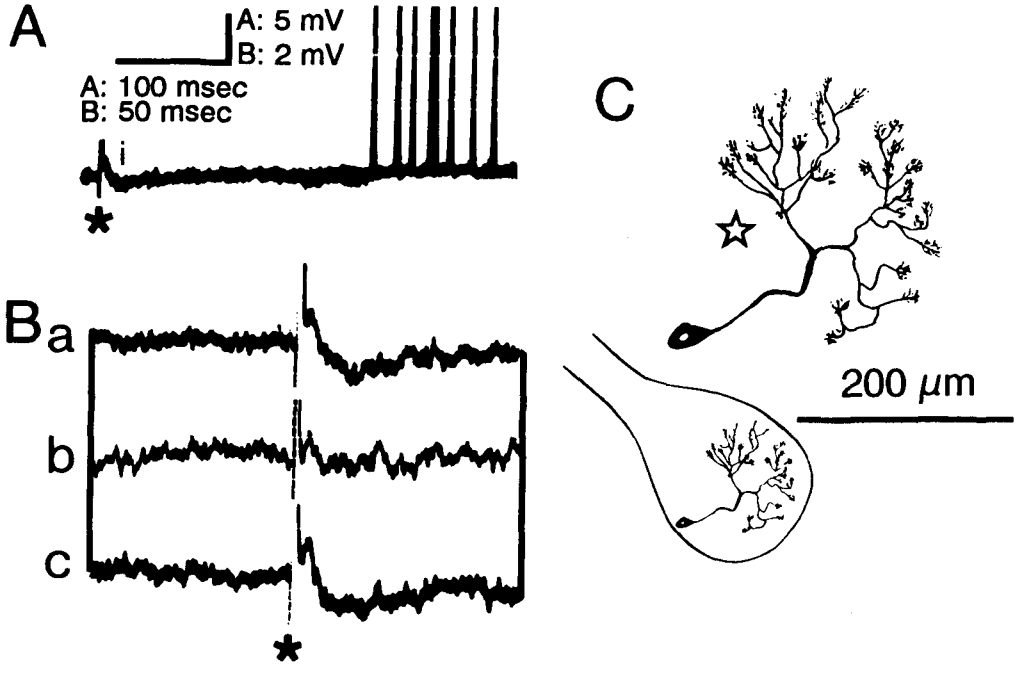

Fig. 8A–C. Delayed-input inhibitory response to electrical stimulation *(asterisks)* of the antennal nerve. **A** Three overlapping traces showing initial IPSP (*i*) and delayed spikes (shown truncated) in response to nerve stimulation. **B** Effect of hyperpolarizing current on IPSP. The IPSP was recorded before (*a*), during (*b*), and after (c) passage of a −0.5-nA current through the recording electrode. Note that the depolarization immediately following the stimulus artifact occurred at a latency shorter than the measured conduction time of 5.5 ms for the antennal nerve and was not affected by hyperpolarizing current. This potential therefore is not a postsynaptic event but more likely an extracellular field potential. **C** Morphology of the neuron as revealed by intracellular staining with Lucifer Yellow CH. This neuron had the same basic "symmetrical" pattern as other LNs already described, but its arborizations were limited and did not extend throughout the AL. Its soma was in the lateral cell group of the AL, and the primary neurite split into 2 major branches that divided further and branched extensively into the dorsal, medial, and ventral glomeruli in the AL. Glomeruli adjacent to the lateral cell group (in the vicinity of the *star*) were not innervated by this LN

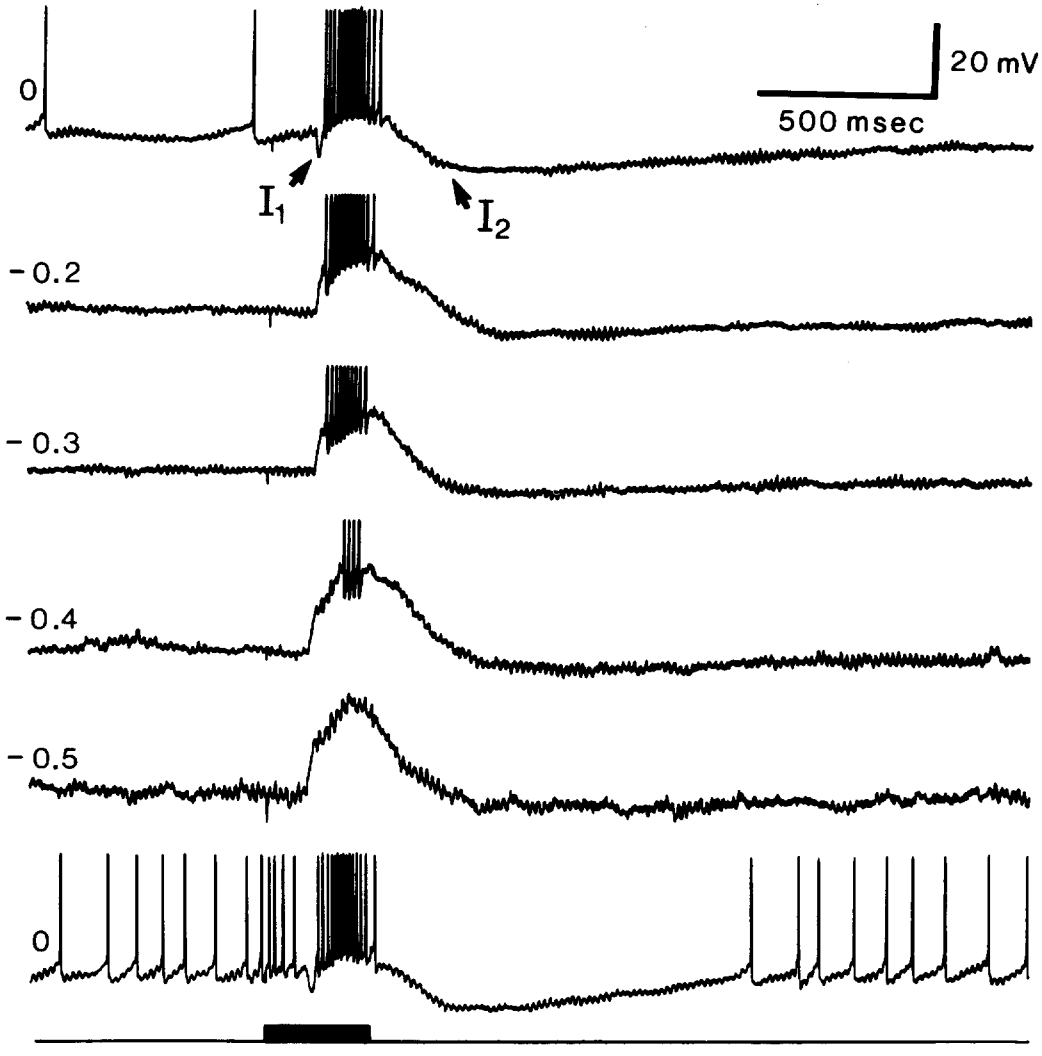

Fig. 9. Effect of hyperpolarizing current on the response of a projection neuron in a male to antennal stimulation with the complete female sex-pheromone blend. Stimulus onset and duration indicated in *bottom trace*. Values at *left* represent amounts of injected current (nA). The early inhibitory potential (I_1) was reversed with only -0.2 nA of injected current (Waldrop et al. 1987), but the delayed hyperpolarization (I_2) was not totally reversed even after injection of -0.5 nA. The amplitude of a compound EPSP underlying the excitatory phase of the response was increased by negative current. Under -0.5 nA of injected current, the fact that I_2 persists in the absence of spike activity suggests that it, like I_1, is mediated through a feed-forward mechanism rather than a feedback pathway

pound IPSP that could be reversed by injection of negative current (Fig. 8, B a–c). The amplitude of spontaneous EPSPs also increased during current injection. Odors were not tested.

Morphology. One neuron of this class was stained intracellularly with Lucifer Yellow (Fig. 8C). This neuron had the same basic "symmetrical" structure observed before, but the dendritic arborizations were restricted to glomeruli in the dorsal, medial, and ventral parts of the AL and did not extend into lateral glomeruli.

Synaptic interactions between LNs and PNs

In order to examine synaptic interactions among AL neurons, 2 electrodes were inserted into the AL neuropil, and pairs of neurons were impaled simultaneously. Only microelectrodes filled with 3 *M* KCl or 2 *M* K-acetate were used in these experiments because the recordings from high-resistance, dye-filled electrodes were often too noisy to permit observations of small postsynaptic potentials. The impaled neurons were therefore characterized

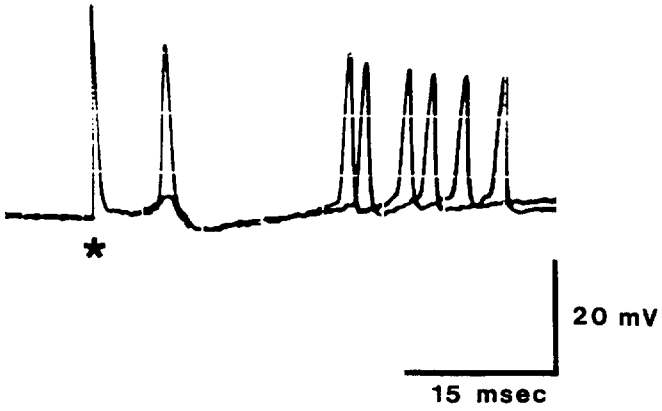

Fig. 10. Response of a PN to electrical stimulation of the antennal nerve *(asterisk)*. Two overlapping traces showing that the time-course and amplitude of I_1 are not affected by a preceding spike (see text)

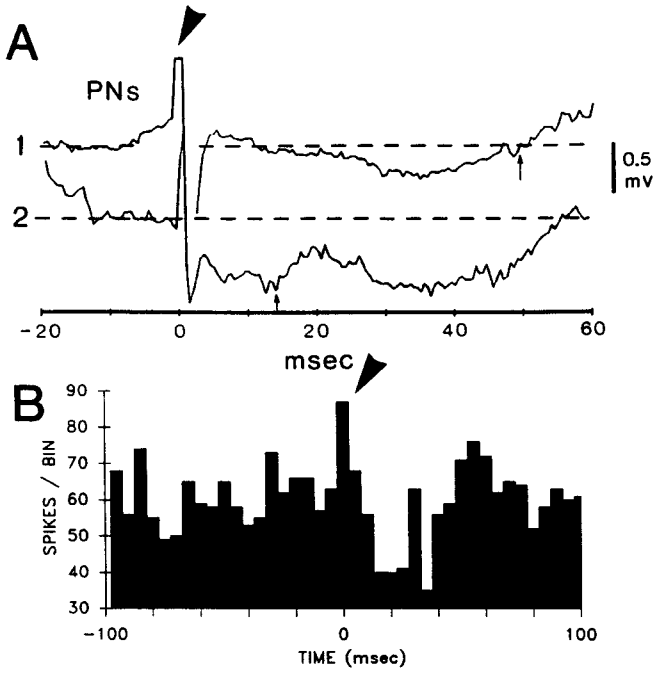

Fig. 11A, B. Spike-triggered averaging and cross-correlation analysis revealed synaptic interactions in LN–PN pairs. **A** Averaged responses in PNs triggered off a spontaneous LN spike at time indicated by *arrowhead.* Spontaneous LN activity elicited a membrane hyperpolarization in PNs. Note that membrane depolarizations were sometimes correlated with the LN spike *(arrows),* but the initial response was a hyperpolarization in all cases ($n=6$). Coupling potential *(arrowhead)* made it impossible to measure the latency of the initial hyperpolarization. Resting membrane potential indicated by *dashed lines.* Average of 225 events in *trace 1* and 260 events in *trace 2.* **B** Cross-correlation analysis in a third pair revealed a period of spike suppression in the PN following the LN spike artifact *(arrowhead).* The period of spike suppression corresponds to the time course of the membrane hyperpolarization shown in **A.** Plot based on 790 LN spikes, 2082 PN spikes, 5-ms bins

on the basis of physiological criteria alone. Reliable characteristics of short-latency LNs were an excitatory, short- (0.5–2 ms) and fixed-latency response to stimulation of the antennal nerve, the appearance of large, relatively broad spikes, and the presence of multiple spike amplitudes, as shown above. A complex response to antennal-nerve stimulation, consisting of inhibitory and excitatory components and impulses of relatively short duration, was used as a reliable indicator of PNs (Fig. 9; Waldrop et al. 1987; Christensen and Hildebrand 1988). The initial phase of the PN response was a brief IPSP (I_1) which preceded excitatory input that elicited firing of impulses. This IPSP was not dependent upon any preceding spike activity. An electrical stimulus of suprathreshold intensity evoked an IPSP with a time course identical to that evoked by a subthreshold stimulus (Fig. 10). A delayed and much prolonged hyperpolarizing phase (I_2) often followed the period of firing in PNs (Fig. 9). This later I_2 phase also had an apparent reversal potential different from that of I_1 (Fig. 9).

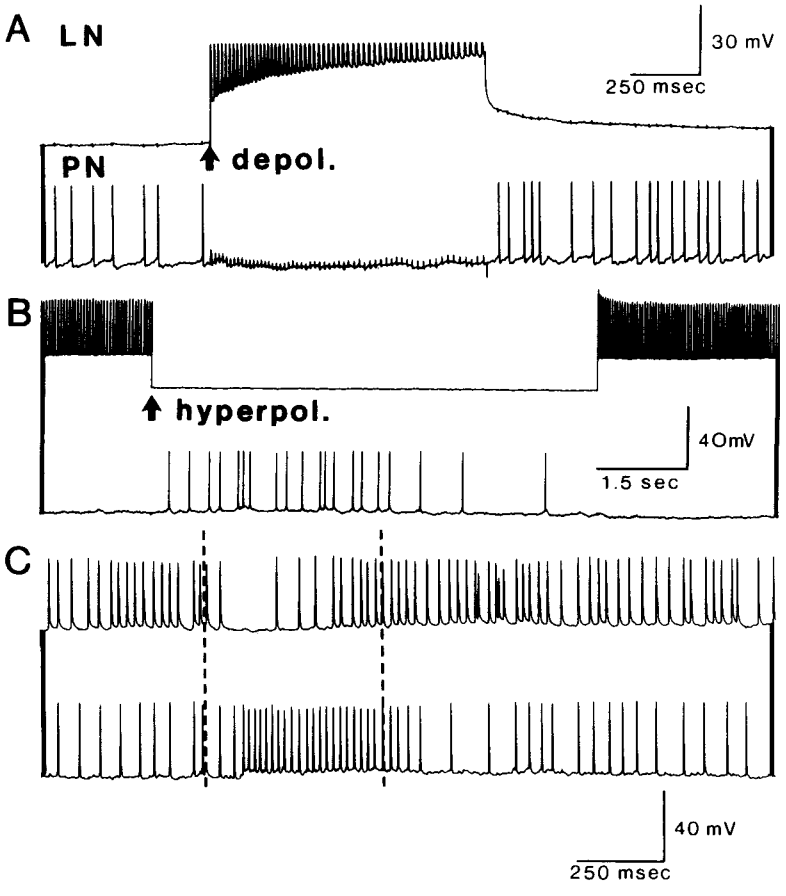

Fig. 12A–C. Examples of interactions in 3 LN–PN pairs. In each case, spike-triggered averaging revealed that the PN was inhibited as a consequence of LN firing, as shown in Fig. 11. **A** Current-induced firing in the LN led to hyperpolarization and suppression of firing in the PN (monitored simultaneously). Small deflections in the PN record are coupling artifacts from LN spikes. The time-course of the PN suppression closely followed the period of current injection in the LN, and spiking in the PN resumed immediately upon repolarization of the LN. **B** Hyperpolarizing current injected into another LN caused an abrupt suppression of firing, and this resulted in depolarization and the release of firing in the PN. This firing in the PN occurred only during the LN hyperpolarization. The excitation in the PN may thus have been mediated through disinhibition. **C** Odor-induced responses recorded simultaneously from an LN and a PN that was inhibited by the LN. When the ipsilateral antenna was stimulated with the principal sex-pheromone component, bombykal, the LN was inhibited, and firing was suppressed. Suppression of firing in the LN was associated with increased firing in the PN, again suggesting that the PN was depolarized through disinhibition. The period of elevated PN activity closely approximated the duration of the stimulus (marked by *dashed lines*)

We impaled 30 LN–PN pairs and observed clear synaptic interactions between neurons in 6 cases (Fig. 11). Subthreshold activity in the LN could not be correlated with postsynaptic activity in the PN. Only the large-amplitude spikes in the LN elicited detectable activity in the PN. Furthermore, all interactions were unidirectional, from LN to PN, and the responses of PNs were always inhibitory. Analysis of PN activity by spike-triggered averaging revealed a small but consistent hyperpolarization that was phase-locked to the spontaneous LN trigger spike (Fig. 11A). Unfortunately, the coupling potential (LN spike reflected in the closely-placed PN electrode) precluded accurate latency measurements. Cross-correlation analysis showed that a period of suppression of firing in the PN was phase-locked to the LN spike, and this period had a time course similar to those of the hyperpolarization shown in Fig. 11A and the antennal nerve-evoked early IPSP I_1 shown in Fig. 9.

In each of the 3 LN–PN pairs shown in Fig. 12, spontaneous LN activity inhibited the PN as in Fig. 11. The LN–PN interactions were greatly enhanced, however, by injection of current into the LN. A current-induced train of impulses in the LN led to membrane hyperpolarization and complete suppression of background activity in the PN (Fig. 12A). Firing of the PN resumed as soon as current injection was stopped and the LN membrane repolarized. The dependence of PN activity on LN activity was further tested by hyperpolarization of a LN that was already firing. Injection of negative current into the LN stopped the firing (Fig. 12B), resulting in a release of activity in the previously inactive PN.

These results suggest that LNs may exert a tonic inhibitory influence over PNs and that at least some apparent excitation of PNs may be mediated through disinhibition. Further evidence for such disinhibition arose when we examined the responses of an LN–PN pair in a male AL to stimulation of the antenna with sex pheromone. The principal component of the sex pheromone, bombykal, caused hyperpolarization and suppression of background firing activity in one LN that inhibited a PN (Fig. 12C). Suppression of firing in the LN led to activation of firing in the PN, again suggesting that the PN was depolarized through disinhibition. It is notable that throughout the records, activity in the LN was mirrored by relative inactivity in the PN.

Discussion

Approximately one-third of the neurons in the AL of *M. sexta* are LNs (Homberg et al. 1989). In spite of their relative abundance, however, little is known about the role(s) of LNs in the processing of olfactory information in the AL. Earlier studies suggested that LNs receive direct synaptic input from axons of antennal olfactory receptor neurons (Tolbert and Hildebrand 1981), as also has been demonstrated in the cockroach *Periplaneta americana* (Boeckh et al. 1989; Distler 1990a, b). The results of our experiments involving electrical and olfactory stimulation of the antennal nerve support that conclusion, but it may not apply to all types of LNs in the AL. On the basis of physiological evidence from intracellular recordings, it appears that antennal sensory axons made direct excitatory synaptic connections with about 82% (71/86) of the LNs examined in this study. Another 13% (11/86) were characterized by delayed excitatory input, and the remaining 5% (4/86) received delayed inhibitory input (Table 1). Furthermore, the first 2 response patterns are not monophasic: excitatory responses in LNs are followed by a membrane hyperpolarization, indicating the participation of additional cellular or synaptic mechanisms. The 3 response categories we have described here do not necessarily represent 3 distinct cell classes. It is certainly possible that the different electrical properties we observed simply reflect different penetration sites in the neuropil and differences in the active and passive properties of the LN membrane (see below). This diversity of postsynaptic response patterns exhibited by LNs nevertheless suggests that these neurons are involved in a variety of local-circuit interactions that influence the output from the AL.

Based on previous findings as well as our present results, our working hypothesis is that one major function of LNs is to provide inhibitory synaptic input to PNs, the output neurons that transmit information from the AL to the protocerebrum. Most, if not all, of the ca. 360 wide-field (multiglomerular) LNs in the AL are GABA-immunoreactive (Hoskins et al. 1986; Homberg et al. 1989), and several lines of physiological evidence indicate that they are inhibitory. First, a complex postsynaptic response including inhibitory phases is elicited in PNs in response to electrical or olfactory stimulation of the primary-afferent input to the AL. The initial compound IPSP (I_1 in Fig. 9), which is observed in all PNs with arborizations in ordinary glomeruli and in some PNs with arborizations in the MGC (see below), is associated with an increased conductance to Cl^- ions, blocked reversibly by bicuculline methiodide and picrotoxin, and mimicked by application of GABA or the GABA agonist muscimol (Waldrop et al. 1987). The strongest evidence that LNs mediate I_1 in the PN response comes from the finding, reported in this paper, that the background activity of a single LN is sufficient to elicit a small hyperpolarization with a time course similar to that of I_1 as recorded in PNs (compare Fig. 9 with Fig. 11). The synchronous, parallel activation of many LNs, as occurs with a natural odor stimulus, should therefore suffice to elicit I_1, which in most PNs is typically 10–15 mV in amplitude. Similarly, we would expect the duration of I_1 elicited by a normal odor stimulus to be shorter than the hyperpolarizing potentials shown in Fig. 11A, owing to the concurrent activation of excitatory input to the PN (Fig. 9).

Factors affecting the synaptic output from LNs

The fact that we did not find interactions between all LN–PN pairs suggests several possible factors that may limit interactions between LNs and PNs, and may further offer some insight into the complex organization of this neuropil. One possibility is that individual PNs may not

receive synaptic input from certain LNs. For example, because the arborizations of some LNs are clearly restricted to particular parts of the AL (Kanzaki and Shibuya 1986; Flanagan and Mercer 1989a; Fig. 4D in this study), these LNs apparently interact synaptically with only a subset of PNs. Alternatively, a lack of observed LN–PN interactions might be attributable to the active and passive properties of different regions of the LN membrane. Although most LNs display wide-field branching throughout the AL (Fig. 4A), individual neuritic branches may be electrically isolated from others, and activity in such isolated "compartments" of the LN might cause a change only in the local circuits within a single glomerulus or a small subset of glomeruli. Evidence for such compartmentalization is apparent during the antennal nerve-evoked hyperpolarization of the LN shown in Fig. 2A. As the membrane repolarized, the small-amplitude spikes recovered well before the large-amplitude spikes. This finding supports the idea that these 2 types of action potentials may be generated in different regions of the same neuron (Matsumoto and Hildebrand 1981) and that LNs function as "multiplex" neurons, as shown in a number of other systems (e.g. Llinas and Sugimori 1980; Tauc and Hughes 1963; Waxman 1972). Whether a given LN is involved in transmission of information throughout the AL or to only a few glomeruli depends upon the neuron's membrane properties at any given time. Mechanisms for modulating the cable properties of LNs, which could be involved in regulation of excitability and information flow in the AL, are currently under investigation (Kloppenburg and Hildebrand 1992; Mercer et al. 1992; Sun et al. 1992). Centrifugal input to the AL could play a role in this modulation (Ernst and Boeckh 1983; Homberg et al. 1989).

Synaptic interactions in the glomerular neuropil

Simultaneous intracellular recordings from LN–PN pairs has permitted the following observations: (1) firing, either spontaneous or current-induced, in the LN led to a postsynaptic response in the PN in 20% of the pairs studied; (2) activity in the LN always suppressed activity in the PN; (3) no reciprocal interactions (i.e., from PN to LN) were detected; and (4) decreased firing of the LN (either current- or odor-induced) caused an increase in firing of the PN, suggesting that LNs tonically inhibit PNs. These findings also suggest that at least some polysynaptic "excitation" of PNs may be due to a disinhibitory circuit involving 2 inhibitory LNs. Ultrastructural examination of the AL neuropil in *M. sexta* has revealed serial synapses (Tolbert and Hildebrand 1981; Distler 1990b; Malun 1991b), but the identities of the synaptic elements involved in those structures have not yet been determined. Our present observations show that the antennal nerve-evoked response of LNs typically includes a delayed inhibitory component (Figs. 2, 5 and 8). This input could come from another inhibitory LN. Recently, ultrastructural evidence from the cockroach AL demonstrated a synaptic contact between 2 LNs that both exhibited GABA-like immunoreactivity (Boeckh et al. 1990).

Disinhibition is only one possible mechanism for generating a depolarizing response in PNs, however. A small depolarizing "bump" sometimes precedes I_1 in the response evoked in PNs by electrical stimulation of the antennal nerve (Fig. 10), and at greater stimulus intensities, this small initial depolarization can trigger a spike. In most PNs, this depolarization is unaffected by injection of current and shows rapid decrement during repetitive stimulation at 5 Hz (Waldrop et al. 1987). These findings therefore suggest a polysynaptic pathway from primary afferents to PNs. Further examination of these possible synaptic relationships is needed before we can understand how excitatory responses in PNs are generated.

Functions of LNs in olfactory information processing

Our findings indicate that some LNs reverse the sign of the incoming olfactory information through putatively GABAergic inhibitory synapses. One possible role for the inhibitory LNs is to mediate lateral inhibition between glomeruli. Such a mechanism could serve to enhance olfactory signals within one glomerulus while simultaneously reducing excitability within the surrounding glomeruli and thus raising the signal-to-noise ratio in the system. Output synapses from the larger processes of PNs onto GABA-immunoreactive neurites in the glomerular neuropil have been found in the cockroach AL (Malun 1991a, b), and these connections could mediate such lateral inhibitory interactions. In 3 experiments, however, we did not observe any interactions between pairs of PNs separated by ca. 250 μm in the AL of *M. sexta*. Thus the activity of a PN in one part of the AL appeared not to have an effect on the activity of another PN elsewhere in the AL. It remains to be seen whether PNs of the same or adjacent glomeruli exhibit interactions through intercalated LNs, but such recordings are extremely difficult to obtain.

Another possible role for LNs is to permit the system to monitor accurately the dynamic temporal characteristics of olfactory stimuli. Our findings show that LNs often are active spontaneously (Fig. 1), whereas PNs typically remain quiescent in the absence of antennal afferent input (Christensen and Hildebrand 1987, 1988; Waldrop et al. 1987; Kanzaki et al. 1989; Hansson et al. 1991). This suggests that the several hundred LNs that converge in each glomerulus (Homberg et al. 1989) may exert a tonic inhibitory influence over spontaneous PN activity (Fig. 12). This action would help ensure that background activity does not obscure the temporal pattern of the excitatory response mediated by an olfactory input to the PN.

LNs also may be involved in generating responses in PNs to the conspecific sex-pheromone blend, which in *M. sexta* comprises 8 C_{16}-aldehydes, 2 of which are necessary and sufficient to evoke the male moth's characteristic behavioral responses to the female's sex pheromone (Tumlinson et al. 1989). A specific subpopulation

of PNs associated with the MGC of male *M. sexta* (Fig. 9) can encode each stimulus pulse with a discrete burst of spikes (Christensen and Hildebrand 1988). The ability to perform this task, however, depends upon the nearly synchronous integration of convergent excitatory and inhibitory input to the PN. One of the 2 essential pheromone components elicits depolarization of the PN, while the other essential component is responsible for the initial hyperpolarization, I_1 (Christensen and Hildebrand 1987b; Fig. 9). It is likely that inhibitory LNs participate in one or both of these initial phases of this complex postsynaptic response and contribute to the neuron's ability to monitor accurately the behaviorally significant discontinuities in the pheromonal stimulus (Christensen and Hildebrand 1988). The separation between spike bursts is further enhanced by another inhibitory component (I_2 in Fig. 9), which differs from I_1 in several important respects. Unlike I_1, I_2 is relatively insensitive to bicuculline methiodide and picrotoxin (Waldrop et al. 1987), and it has a different apparent reversal potential (Fig. 9). These observations suggest that I_2 may be due to a synaptic mechanism different from the GABA-mediated Cl^- conductance believed to underlie I_1 and that the LNs that receive a delayed excitatory input (Figs. 5–7) may be involved in this delayed inhibition. Its relative insensitivity to current injection may also imply that I_2 is generated in the more distal neurites of the PNs, which presumably are electrically more remote from the site of current injection. Acetylcholine injected into the neuropil of the AL evokes strong and prolonged inhibition in some AL neurons (Waldrop and Hildebrand 1989) and thus could be a neurotransmitter mediating I_2. Other possible neurotransmitter candidates include the various neuropeptides that are colocalized with GABA in certain subsets of LNs (Homberg et al. 1989). A closer examination of the mechanisms that produce I_2 in PNs is required to determine its origins.

Phylogenetic comparisons

Our physiological observations allow us to make certain inferences about the synaptic organization of the AL neuropil in *M. sexta,* and these ideas become even more compelling when our findings are compared with those obtained in studies of the vertebrate olfactory bulb (OB). When the antennal nerve is stimulated electrically, the synaptic responses recorded from certain LNs in *M. sexta* bear a striking similarity to those recorded from local elements in the OB (Wellis and Scott 1990). Likewise, the responses recorded from AL PNs are remarkably similar to those recorded from the principal output elements in the OB, the mitral and tufted cells (Hamilton and Kauer 1988). A comparison of these responses points to the possibility that the synaptic circuits of the AL and the OB may be organized similarly and share many of the same operating principles. It seems appropriate, for example, to draw an analogy to the well known case of reciprocal dendrodendritic synapses between mitral/tufted and granule cells in the vertebrate OB to help explain the inhibition of PNs in the moth AL. Careful examination of our evidence, however, shows that this analogy is not entirely valid. Neither I_1 nor I_2 required even a single spike to precede it (Christensen and Hildebrand 1987b; Waldrop et al. 1987; Fig. 9), and the presence of a spike preceding I_1 did not augment the inhibitory response (Fig. 10). Furthermore, subthreshold activity in LNs was not sufficient to hyperpolarize PNs, and the activity of PNs had no apparent effect on LN activity recorded simultaneously. These results indicate that the inhibitory potentials I_1 and I_2 in PNs are mediated by interneurons that participate in lateral or feed-forward inhibitory pathways, and not feedback pathways. Feed-forward inhibition is also responsible for generation of the hyperpolarizing potentials in mitral/tufted cells in the vertebrate OB (Getchell and Shepherd 1975a, b; Mori 1987; Hamilton and Kauer 1988, 1989; Wellis et al. 1989) and in pyramidal cells in rat hippocampus (Alger and Nicoll 1982; Newberry and Nicoll 1984; Ashwood et al. 1984). Reciprocal synaptic connections have been found in the AL neuropil of both cockroaches (Boeckh et al. 1990) and honeybees (Gascuel and Masson 1991), but these contacts are rare and their function is unknown, unlike the case in the vertebrate OB. In *M. sexta,* there is neither anatomical nor physiological evidence for the self-inhibition of PNs that is commonly observed in vertebrate mitral/tufted cells, and it seems that feed-forward inhibitory pathways play a major role in shaping the output from AL glomeruli.

Our findings reveal important aspects of the central olfactory circuitry involved in processing odors in the moth's environment. Axons of olfactory receptor cells have direct synaptic connections to most LNs and possibly indirect excitatory and inhibitory connections with others. This divergent pattern of connectivity insures that olfactory information is distributed to a diverse population of LNs with a range of different integrative properties involving multicomponent synaptic connections. By contributing to both the excitatory and inhibitory phases of the antennal nerve-evoked postsynaptic responses in PNs, LNs play key roles in generating the patterned output from the olfactory glomeruli. Confirmation of the various synaptic connections proposed for the glomerular neuropil of the AL in *M. sexta* now requires the use of ultrastructural techniques that allow the unambiguous identification of pre- and postsynaptic elements in the complex synaptic ensembles of the glomerular neuropil (Tolbert and Hildebrand 1981; Boeckh and Tolbert 1993).

Acknowledgements. We thank Peggy Randolph for technical assistance; Charles A. Hedgcock, R.B.P., for photographic assistance; A.A. Osman for insect rearing; and Drs. Edmund Arbas, Cole Gilbert, Jon Hayashi, and Leslie Tolbert for helpful discussions and comments on the manuscript. Drs. James Buckner and James Svoboda of the U.S.D.A. generously provided *Manduca sexta* eggs, and Dr. James H. Tumlinson of the U.S.D.A. kindly supplied synthetic sex-pheromone components. This research was supported by NIH grants AI–17711 and AI–23253 (to J.G.H.).

References

Alger BE, Nicoll RA (1982) Feed-forward dendritic inhibition in rat hippocampal pyramidal cells studied *in vitro*. J Physiol (Lond) 328:105–123

Arnold G, Budharugsa S, Masson C (1988) Organization of the antennal lobe in the queen honeybee, *Apis mellifera* L. (Hymenoptera: Apidae). Int J Insect Morphol Embryol 17:185–195

Ashwood TJ, Lancaster B, Wheal HV (1984) *In vivo* and *in vitro* studies on putative interneurones in the rat hippocampus: possible mediators of feed-forward inhibition. Brain Res 293:279–291

Boeckh J, Boeckh V (1979) Threshold and odor specificity of pheromone-sensitive neurons in the deutocerebrum of *Antheraea pernyi* and *A. polyphemus*. J Comp Physiol 132:235–242

Boeckh J, Ernst KD (1987) Contribution of single unit analysis in insects to an understanding of olfactory function. J Comp Physiol A 161:549–565

Boeckh J, Tolbert LP (1993) Synaptic organization and development of the antennal lobe in insects. Microsc Res Tech 24:260–280

Boeckh J, Ernst KD, Selsam P (1989) Double labelling reveals monosynaptic connection between antennal receptor cells and identified local interneurons in the deutocerebrum in the American cockroach. Zool Jb Anat 119:303–312

Boeckh J, Distler P, Ernst KD, Hösl M, Malun D (1990) Olfactory bulb and antennal lobe. In: Schild D (ed) Chemosensory information processing. Springer, Berlin Heidelberg New York, pp 201–227

Burrows M, Boeckh J, Esslen J (1982) Physiological and morphological properties of interneurones in the deutocerebrum of male cockroaches which respond to female pheromone. J Comp Physiol 145:447–457

Christensen TA, Hildebrand JG (1986) Synaptic relationships between local and projection neurons in the antennal lobe of the sphinx moth *Manduca sexta*. Soc Neurosci Abstr 12:857

Christensen TA, Hildebrand JG (1987a) Functions, organization, and physiology of the olfactory pathways in the lepidopteran brain. In: Gupta AP (ed) Arthropod brain: its evolution, development, structure and functions. Wiley, New York, pp 457–484

Christensen TA, Hildebrand JG (1987b) Male-specific, sex pheromone-selective projection neurons in the antennal lobes of the moth *Manduca sexta*. J Comp Physiol A 160:553–569

Christensen TA, Hildebrand JG (1988) Frequency coding by central olfactory neurons in the sphinx moth *Manduca sexta*. Chemical Senses 13:123–130

Christensen TA, Hildebrand JG (1990) Representation of sex-pheromonal information in the insect brain. In: Døving KB (ed) Proc Xth Internatl Symp Olfaction and Taste (ISOT X). Graphic Communication Systems, Oslo, pp 142–150

Christensen TA, Mustaparta H, Hildebrand JG (1989a) Discrimination of sex pheromone blends in the olfactory system of the moth. Chemical Senses 14:202–217

Christensen TA, Hildebrand JG, Tumlinson JH, Doolittle RE (1989b) The sex pheromone blend of *Manduca sexta:* responses of central olfactory interneurons to antennal stimulation in male moths. Arch Insect Biochem Physiol 10:281–291

Christensen TA, Mustaparta H, Hildebrand JG (1991) Chemical communication in heliothine moths. II. Central processing of intra- and interspecific olfactory messages in the male corn earworm moth *Helicoverpa zea*. J Comp Physiol A 169:259–274

Distler P (1989) Histochemical demonstration of GABA-like immunoreactivity in cobalt labeled neuron individuals in the insect olfactory pathway. Histochemistry 91:245–249

Distler P (1990a) Synaptic connections of dopamine-immunoreactive neurons in the antennal lobes of *Periplaneta americana*. Colocalization with GABA-like immunoreactivity. Histochemistry 93:401–408

Distler P (1990b) GABA-immunocytochemistry as a label for identifying types of local interneurons and their synaptic contacts in the antennal lobes of the American cockroach. Histochemistry 93:617–626

Ernst KD, Boeckh J (1983) A neuroanatomical study on the organization of the central antennal pathways in insects. III. Neuroanatomical characterization of physiologically defined response types of deutocerebral neurons in *Periplaneta americana*. Cell Tissue Res 229:1–22

Flanagan D, Mercer AR (1989a) Morphology and response characteristics of neurones in the deutocerebrum of the brain in the honeybee *Apis mellifera*. J Comp Physiol A 164:483–494

Flanagan D, Mercer AR (1989b) An atlas and 3-D reconstruction of the antennal lobes in the worker honeybee, *Apis mellifera* L. (Hymenoptera: Apidae). Int J Insect Morphol Embryol 18:145–159

Gascuel J, Masson C (1991) A quantitative ultrastructural study of the honeybee antennal lobe. Tissue Cell 23:341–355

Getchell TV, Shepherd GM (1975a) Synaptic actions on mitral and tufted cells elicited by olfactory nerve volleys in the rabbit. J Physiol (Lond) 251:497–522

Getchell TV, Shepherd GM (1975b) Short-axon cells in the olfactory bulb: dendrodendritic synaptic interactions. J Physiol (Lond) 251:523–548

Hamilton KA, Kauer JS (1988) Responses of mitral/tufted cells to orthodromic and antidromic electrical stimulation in the olfactory bulb of the tiger salamander. J Neurophysiol 59:1736–1755

Hamilton KA, Kauer JS (1989) Patterns of intracellular potentials in salamander mitral/tufted cells in response to odor stimulation. J Neurophysiol 62:609–625

Hansson BS, Christensen TA, Hildebrand JG (1991) Functionally distinct subdivisions of the macroglomerular complex in the antennal lobe of the male sphinx moth *Manduca sexta*. J Comp Neurol 312:264–278

Homberg U (1984) Processing of antennal information in extrinsic mushroom body neurons of the bee brain. J Comp Physiol A 154:825–836

Homberg U, Montague RA, Hildebrand JG (1988) Anatomy of antenno-cerebral pathways in the brain of the sphinx moth *Manduca sexta*. Cell Tissue Res 254:255–281

Homberg U, Christensen TA, Hildebrand (1989) Structure and function of the deutocerebrum in insects. Anu Rev Entomol 34:477–501

Hoskins SG, Homberg U, Kingan TG, Christensen TA, Hildebrand JG (1986) Immunocytochemistry of GABA in the antennal lobes of the sphinx moth *Manduca sexta*. Cell Tissue Res 244:243–252

Hösl M (1990) Pheromone-sensitive neurons in the deutocerebrum of *Periplaneta americana:* receptive fields on the antenna. J Comp Physiol A 167:321–327

Kanzaki R, Shibuya T (1986) Identification of the deutocerebral neurons responding to the sexual pheromone in the male silkworm moth brain. Zool Sci 3:409–418

Kanzaki R, Arbas EA, Strausfeld NJ, Hildebrand JG (1989) Physiology and morphology of projection neurons in the antennal lobe of the male moth *Manduca sexta*. J Comp Physiol A 165:427–453

Kingan TG, Hildebrand JG (1985) γ-Aminobutyric acid in the central nervous system of metamorphosing and mature *Manduca sexta*. Insect Biochem 15:667–675

Kloppenburg P, Hildebrand JG (1992) Modulatory effects of 5-hydroxytryptamine on interneurons in the antennal lobe of the sphinx moth *Manduca sexta*. Soc Neurosci Abstr 18:303

Light DM (1986) Central integration of sensory signals: an exploration of processing of pheromonal and multimodal information in lepidopteran brains In: Payne TL, Birch MC, Kennedy CEJ (eds) Mechanisms in insect olfaction. Oxford Univ Press, Oxford, pp 287–301

Llinás R, Sugimori M (1980) Electrophysiological properties of *in vitro* Purkinje cell dendrites in mammalian cerebellar slices. J Physiol (Lond) 305:197–213

Malun D (1991a) Synaptic relationships between GABA-immunoreactive neurons and an identified uniglomerular projection neuron in the antennal lobe of *Periplaneta americana:* a double-labeling electron microscopic study. Histochemistry 96:197–207

Malun D (1991b) Inventory and distribution of synapses of identified uniglomerular projection neurons in the antennal lobe of *Periplaneta americana.* J Comp Neurol 305:348–360

Masson C, Mustaparta H (1990) Chemical information processing in the olfactory system of insects. Physiol Rev 70:199–245

Matsumoto SG, Hildebrand JG (1981) Olfactory mechanisms in the moth *Manduca sexta:* response characteristics and morphology of central neurons in the antennal lobes. Proc R Soc Lond B 213:249–277

Mercer AR, Hayashi JH, Hildebrand JG (1992) Modulatory effects of 5-hydroxytryptamine on voltage-gated currents in cultured insect olfactory neurons. Soc Neurosci Abstr 18:303

Mori K (1987) Membrane and synaptic properties of identified neurons in the olfactory bulb. Prog Neurobiol 29:275–320

Newberry NR, Nicoll RA (1984) A bicuculline-resistant inhibitory post-synaptic potential in rat hippocampal pyramidal cells *in vitro.* J Physiol (Lond) 348:239–254

Olberg RM (1983) Interneurons sensitive to female pheromone in the deutocerebrum of the male silkworm moth, *Bombyx mori.* Physiol Entomol 8:419–428

Pichon Y, Sattelle DB, Lane NJ (1972) Conduction processes in the nerve cord of the moth *Manduca sexta* in relation to its ultrastructure and haemolymph ionic composition. J Exp Biol 56:717–734

Rospars JP (1988) Structure and development of the insect antennodeutocerebral system. Int J Insect Morphol Embryol 17:243–294

Schäfer S, Bicker G (1986) Distribution of GABA-like immunoreactivity in the brain of the honeybee. J Comp Neurol 246:287–300

Selzer R (1979) Morphological and physiological identification of food odour specific neurones in the deutocerebrum of *Periplaneta americana.* J Comp Physiol 134:159–163

Starratt AN, Dahm KH, Allen N, Hildebrand JG, Payne TL, Röller H (1979) Bombykal, a sex pheromone of the sphinx moth *Manduca sexta.* Z Naturforsch 34C:9–12

Stocker RF, Lienhard MC, Borst A, Fischbach K-F (1990) Neuronal architecture of the antennal lobe in *Drosophila melanogaster.* Cell Tissue Res 262:9–34

Sun XJ (1991) Caractérisation électrophysiologique et morphologique des neurones olfactifs du lobe antennaire de l'abeille, *Apis mellifera.* D Sc thesis, Université de Paris-Sud, Centre d'Orsay, France, pp 1–184

Sun XJ, Tolbert LP, Hildebrand JG (1992) Ultrastructural characteristics of the 5HT-immunoreactive neuron in the antennal lobe of *Manduca sexta.* Soc Neurosci Abstr 18:303

Tauc L, Hughes GM (1963) Modes of initiation and propagation of spikes in the branching axons of molluscan central neurons. J Gen Physiol 46:533–549

Tolbert LP, Hildebrand JG (1981) Organization and synaptic ultrastructure of glomeruli in the antennal lobes of the moth *Manduca sexta:* a study using thin sections and freeze-fracture. Proc R Soc Lond B 213:279–301

Tumlinson JH, Brennan MM, Doolittle RE, Mitchell ER, Brabham A, Mazomenos BE, Baumhover AH, Jackson DM (1989) Identification of a pheromone blend attractive to *Manduca sexta* (L.) males in a wind tunnel. Arch Insect Biochem Physiol 10:255–271

Waldrop B, Hildebrand JG (1989) Physiology and pharmacology of acetylcholinergic responses of interneurons in the antennal lobes of the moth *Manduca sexta.* J Comp Physiol A 164:433–441

Waldrop B, Christensen TA, Hildebrand JG (1987) GABA-mediated synaptic inhibition of projection neurons in the antennal lobes of the sphinx moth *Manduca sexta.* J Comp Physiol A 161:23–32

Waxman SG (1972) Regional differentiation of the axon: A review with special reference to the concept of the multiplex neuron. Brain Res 47:269–288

Wellis DP, Scott JW (I990) Intracellular responses of identified rat olfactory bulb interneurons to electrical and odor stimulation. J Neurophysiol 64:932–947

Wellis DP, Scott JW, Harrison TA (1989) Discrimination among odorants by single neurons of the rat olfactory bulb. J Neurophysiol 61:1161–1177